

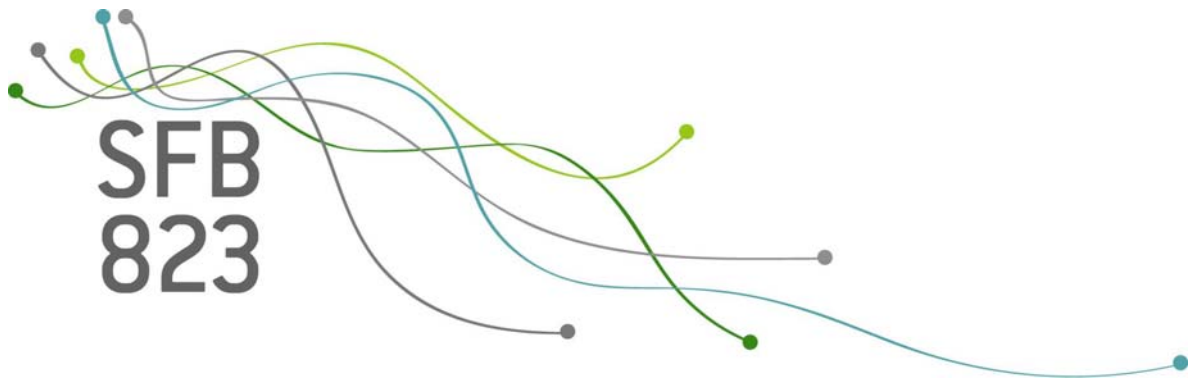
SFB
823

Modelling wear degradation in cylinder liners

Simone Hermann, Fabrizio Ruggeri

Nr. 6/2016

Discussion Paper



Modelling Wear Degradation in Cylinder Liners

Simone Hermann*, Fabrizio Ruggeri†

January 25, 2016

We present and discuss a stochastic model describing the wear process of cylinder liners in a marine diesel engine. The model is based on a stochastic differential equation and Bayesian inference is illustrated. Corrosive action and measurement error, both quite negligible, are modeled with a Wiener process whereas a jump process is used to describe the contribution of soot particles to the wear process. The model can be used to forecast the wear process and, consequently, plan condition based maintenance activities. In the paper, we provide a critical illustration of the mathematical and computational aspects of the model. We propose a strategy that, implemented for simulated and real data, allows for stable parameter estimation and forecasts.

Keywords: Bayesian inference; Condition based maintenance; Markov chain Monte Carlo; Stochastic differential equations.

1 Introduction

Data from a leading Italian ship company are available about the wear process of liners protecting cylinders in marine diesel engines; the thickness of the liner walls is 100 millimeters. The wear process is kept under control through measurements performed using a micrometer in a place, called Top Dead Center, in the top region of the cylinder liner where the maximum wear usually occurs because of high thermomechanical and tribological stresses. Excessively worn cylinder liners are among the major causes of failures of heavy-duty diesel engines; in fact, almost all failures occur once the wear exceeds a specified threshold. The wear is mostly caused by abrasive particles (soot) on the piston surface, produced by the combustion of heavy fuels and oil degradation. Such wear occurs when the lubricant film thickness is less than the soot particle size, so that the soot is involved in a three-body abrasive action with the piston surface on one side and the liner metal surface on the other. The wear occurs

*TU Dortmund University, Faculty of Statistics, Vogelpothsweg 87, D-44221 Dortmund, Germany; hermann@statistik.tu-dortmund.de

†IMATI CNR, Milano, Italy; fabrizio@mi.imati.cnr.it

because the soot particles are harder than the corresponding engine parts. In addition to the abrasive wear, there is a corrosive one due to sulphuric acid, nitrous/nitric acids and water.

The paper presents a stochastic model of the wear process, describing the time evolution of the thickness of the liner at the Top Dead Center. The model is based on a stochastic differential equation which accounts for both abrupt changes in thickness due to abrasive wear and minor ones due to corrosive wear; the former will be considered through a jump process whereas the latter will be modeled with a Wiener process, accounting also for measurement errors.

The major interest for the ship company is in performing a condition based maintenance, aimed to replace liners before the wear exceeds the threshold (4 millimeters) for which the warranty clauses make the ship owner responsible, in lieu of the liner manufacturer, for the costs due to cylinder failures. Other relevant economic aspects are involved, like the costs of stopping ships for inspection and changing liners (approximately 10 meters high). It is therefore important to find a procedure which reduces the number of inspections and avoids early replacements of liners. The stochastic model can be useful in deciding to inspect the ship to check the actual wear when the predicted probability of exceeding the threshold wear at a future time t will be above a fixed value.

Inference on the jump diffusion process will be performed using a Bayesian approach. Full details are provided on the choice of the prior distributions and the Markov chain Monte Carlo (MCMC) scheme which allows computation of posterior quantities of interest and forecasts. In Section 2 we review some of the models used in literature to analyze the data, whereas we discuss the assumptions behind the proposed model in Section 3 and perform a Bayesian analysis in Section 4. Data are analyzed in Section 5 where issues about the choice of prior distributions are discussed and presented also through simulated data. Final remarks and pointers for future research are finally presented in Section 6.

2 Previous works

Bocchetti *et al.* (2006) consider two possible causes of failures in the cylinder liners: the internal wear and the external thermal crack. The wear is caused by the high quantity of abrasive particles on the piston surface, generated by soot due to the combustion of heavy fuels and oil degradation. The thermal crack of the liner is caused by fatigue cracking due to repeated thermal shocks. A thermal shock is caused by abrupt changes in the temperature of the cooling fluid used for the external surface of the liner and is often aggravated by an inadequate chemical treatment of the cooling water. These changes occur mainly during the maneuver operations when it is hard to keep constant the cooling temperature. As a consequence of such shocks, a small crack can arise in the external surface of the liner and then, as the age increases, it propagates towards the inside. Bocchetti *et al.* (2006) consider a competing risk model to describe the failure process of a cylinder liner under the realistic hypotheses that (a) the liner fails when the first of the competing failure mechanisms reaches a failure state, and (b) the failure mechanisms proceed independently of each other. The wear process is described through a stochastic process for which the passage time to a boundary (e.g. the warranty wear limit) is considered as a degradation failure, whereas the failure time due to the thermal crack is modeled via a Weibull distribution. Their study showed that the thermal crack is the dominant failure mode during the first 5000 hours, whereas the wear mechanism dominates from there onward. As a consequence, only wear mechanism is to be

considered when ships are operated for a significantly longer time, as in our case.

In Giorgio *et al.* (2007) the wearing process of a cylinder liner is described by means of a cumulative damage model, where the wearing process is depicted as the accumulation of successive (randomly occurring) isolated injuries. This model is subsequently used for estimating liner reliability (i.e. the probability that the wear will exceed a prefixed threshold), and for developing a condition-based maintenance strategy for the cylinder liners. In particular, they assume that the wear of a cylinder liner at a given age t is the accumulation of isolated injuries (elementary wear) of equal magnitude occurring up to age t . Furthermore, they suppose that the wearing events occur at random time instants, and the probability that an injury occurs in a given time interval is independent of the number of injuries already accumulated. Therefore, wearing events are described by means of a nonhomogeneous Poisson process, namely a Power Law process.

Giorgio *et al.* (2010) introduced a time and state space discretization to obtain the likelihood function of the observed data, considering transition probabilities between process states dependent on the current system state. A step further is taken in Giorgio *et al.* (2011) where the transition probabilities depend not only on the current system state but also on its age. The same authors propose a more sophisticated model based on transformed gamma processes in Giorgio *et al.* (2015a) and apply it in Giorgio *et al.* (2015b) where they formalize and model the optimal maintenance policy in a Decision Analysis framework.

Finally, Moraes *et al.* (2014) considered a multiscale indirect inference methodology for state-dependent Markovian pure jump processes.

The current research is inspired by the work by D’Ippoliti and Ruggeri (2009) who proposed a slightly more complex model but were unable to cope with some computational issues and show the utility of the approach. They considered a jump diffusion process where the Wiener process was mimicking the corrosive wear whereas the abrasive wear was modeled by the jump process. The proposed MCMC algorithm was strongly dependent on the assumption of knowing the number of jumps and their individual sizes between two observed measurements, treating the former as if they were parameters and were generated at each step of the MCMC algorithm. The model had identifiability problems which are addressed in the current paper, first of all considering the jump size as fixed, although unknown, and then developing a strategy based on MCMC chains obtained from many starting points and the removal of those leading to unrealistic values of the parameters.

3 Assumptions

Empirical studies of the wear and the physical properties of the liner lead previous studies, e.g., Bocchetti *et al.* (2006), to observe that the wear increment decreases as a function of wear. As a consequence, the thickness decrement of the cylinder liner also decreases along with thickness. From a physical viewpoint it is known that the background activity of *tiny* particles leads to almost negligible thickness decrements, whereas *large* soot particles are responsible for the most relevant thickness decrements. The proposed model stems from such physical properties.

From a mathematical viewpoint, we consider a stochastic differential equation (SDE) $dX_t = f(X_t)$ to relate the evolution of the thickness X_t over time and its influence on the thickness decrement dX_t . Furthermore, additive accumulation of wear as a sequence of small normally distributed effects, due, e.g., to the *tiny* particles or corrosion, makes reasonable the choice

of a Brownian motion with drift, where the latter is the mean value of the process. Finally, we consider thickness decrement jumps due, possibly, to *large* particles, i.e. the soot, and we model them using a jump process in the SDE.

Based on the latter assumptions on the model, we suppose that the evolution of the thickness process X_t can be described by

$$dX_t = X_t\{\phi dt + \gamma dW_t + \theta dN_t\}, \quad (1)$$

with some constant initial value x_0 and the assumptions $\gamma > 0$ and $\phi, \theta < 0$. Therefore the decrease in thickness is determined by the negative values of the drift ϕ and the jump process which counts the number of jumps of negative size θ , whereas γ should be quite small to avoid unrealistic increments of thickness but, at the same time, take in account both corrosive actions and measurement errors.

For $\theta > -1$ the SDE in (1) has a unique strong solution given by

$$X_t = x_0 \cdot \exp\left(\phi t - \frac{\gamma^2}{2}t + \gamma W_t + \log(1 + \theta)N_t\right). \quad (2)$$

This can be seen by direct calculation using Itô's formula for noncontinuous semimartingales and the result is employed, for example, in Øksendal and Sulem (2005), p. 7 in example 1.15. As a consequence, it is important that the jump size is constrained to $-1 < \theta < 0$ so that a solution of the SDE exists and thickness will decrease over time.

A formula similar to (2) was obtained by D'Ippoliti and Ruggeri about wear at time t during their previously mentioned research. The problem they faced was that the solution at any time t was proportional to the initial wear, i.e. zero. Therefore D'Ippoliti and Ruggeri (2009) considered thickness instead of wear in their model and we are going to do the same in the current paper, although we will sometimes refer to wear in the text.

4 Model and Bayesian analysis

We suppose the thickness of a liner is measured at times $t_1 < \dots < t_n$, providing the observations X_{t_1}, \dots, X_{t_n} . As a consequence of (2), we have that

$$\log(X_{t_i})|N_{t_i}, \phi, \gamma^2, \theta \sim \mathcal{N}(\log(x_0) + (\phi - \frac{\gamma^2}{2})t_i + \log(1 + \theta)N_{t_i}, \gamma^2 t_i), \quad (3)$$

for $i = 1, \dots, n$.

We propose a Bayesian approach where the prior distributions on the parameters in (3) are given by

$$\begin{aligned} N_{t_i} &\sim \mathcal{P}(\lambda t_i), \quad i = 1, \dots, n \\ \phi &\sim \mathcal{N}(m_\phi, v_\phi) \\ \gamma^2 &\sim \mathcal{IG}(a_\gamma, b_\gamma) \\ \tilde{\theta} := \log(1 + \theta) &\sim \mathcal{N}(m_\theta, v_\theta) \\ \lambda &\sim \mathcal{G}(a_\lambda, b_\lambda). \end{aligned} \quad (4)$$

Here $\mathcal{P}, \mathcal{N}, \mathcal{IG}$ and \mathcal{G} denote Poisson, normal, inverse gamma and gamma distributions, respectively.

It is worth mentioning that N_{t_i} , the number of jumps up to time t_i , for $i = 1, \dots, n$, is unobserved and treated as a parameter and, accordingly, generated at each step of the MCMC algorithm. The presence of such *parameter* will make the computations more complex, as well as posing an identifiability problem that we will address in the next sections.

For the partial data vector $\eta = (\phi, \tilde{\theta}, \gamma^2)$, (3) leads to a multivariate normal likelihood for the logarithms

$$(\log(X_{t_1}), \dots, \log(X_{t_n})) | \eta, N_{t_1}, \dots, N_{t_n} \sim \mathcal{N}(\mu_n(\eta), \gamma^2 T_n),$$

where $\mu_n(\eta) = \log(x_0) \cdot \mathbf{1}_n + (\phi - \frac{\gamma^2}{2}) \cdot (t_1, \dots, t_n) + \tilde{\theta} \cdot (N_{t_1}, \dots, N_{t_n})$, $T_n = (\min(t_i, t_j))_{i,j=1,\dots,n}$ and $\mathbf{1}_n = (1, \dots, 1) \in \mathbb{R}^n$. In the following, we denote with $t_{(n)}$ the vector (t_1, \dots, t_n) , with $\log(X)_{(n)}$ the vector $(\log(X_{t_1}), \dots, \log(X_{t_n}))$, and with $N_{(n)}$ the vector $(N_{t_1}, \dots, N_{t_n})$.

Earlier we mentioned that it is important to have $-1 < \theta < 0$ but the choice of a normal prior in (4) for $\tilde{\theta} := \log(1 + \theta)$ seems to be in contradiction with such request since it allows for positive values of $\tilde{\theta}$. Like in other papers, here we exploit the ease of computation induced by the normal distribution and limit the corresponding drawback by an appropriate choice of its parameters so that the probability of positive values is negligible.

Estimation of ϕ and $\tilde{\theta}$ is in fact simplified since the normal prior is conjugate with respect to the multivariate normal likelihood. The full conditional posterior for ϕ is given by

$$\begin{aligned} \phi | \log(X)_{(n)}, N_{(n)}, \tilde{\theta}, \gamma^2 &\sim \mathcal{N}(m_\phi^{\text{post}}, v_\phi^{\text{post}}), \text{ with} \\ v_\phi^{\text{post}} &= \left(\frac{1}{\gamma^2} t_{(n)} T_n^{-1} t_{(n)}^T + \frac{1}{v_\phi} \right)^{-1} \text{ and} \\ m_\phi^{\text{post}} &= v_\phi^{\text{post}} \left\{ \frac{m_\phi}{v_\phi} + \frac{1}{\gamma^2} t_{(n)} T_n^{-1} \left(\log(X)_{(n)} - \log(x_0) \mathbf{1}_n + \frac{\gamma^2}{2} t_{(n)} - \tilde{\theta} N_{(n)} \right)^T \right\}, \end{aligned}$$

whereas for $\tilde{\theta}$ it is given by

$$\begin{aligned} \tilde{\theta} | \log(X)_{(n)}, N_{(n)}, \phi, \gamma^2 &\sim \mathcal{N}(m_\theta^{\text{post}}, v_\theta^{\text{post}}), \text{ with} \\ v_\theta^{\text{post}} &= \left(\frac{1}{\gamma^2} N_{(n)} T_n^{-1} N_{(n)}^T + \frac{1}{v_\theta} \right)^{-1} \text{ and} \\ m_\theta^{\text{post}} &= v_\theta^{\text{post}} \cdot \left\{ \frac{m_\theta}{v_\theta} + \frac{1}{\gamma^2} N_{(n)} T_n^{-1} \left(\log(X)_{(n)} - \log(x_0) \mathbf{1}_n - (\phi - \frac{\gamma^2}{2}) t_{(n)} \right)^T \right\}. \end{aligned}$$

Following from the choice of an inverse gamma prior density $p(\gamma^2) = \frac{b_\gamma}{\mathcal{G}(a_\gamma)} (\gamma^2)^{-a_\gamma-1} \exp\left(-\frac{b_\gamma}{\gamma^2}\right)$, we compute the full conditional posterior density for γ^2 as

$$\begin{aligned} p(\gamma^2 | \log(X)_{(n)}, N_{(n)}, \phi, \tilde{\theta}) \\ \propto (\gamma^2)^{-(\frac{n}{2} + a_\gamma) - 1} \\ \exp\left(-\frac{1}{\gamma^2} \left\{ \frac{1}{2} (\log(X)_{(n)} - \mu_n(\eta)) T_n^{-1} (\log(X)_{(n)} - \mu_n(\eta))^T + b_\gamma \right\}\right). \end{aligned}$$

Since $\mu_n(\eta)$ depends also on γ^2 , the posterior distribution of the latter is not an inverse gamma distribution. In this case we can perform a Metropolis-Hastings (MH) step within

the Gibbs sampler and use the inverse gamma as proposal density. With $\mu_{n,\phi,\tilde{\theta}}(\gamma^2) := \mu_n(\eta)$, we define the proposal density

$$q(\gamma^2|\tilde{\gamma}^2, \phi, \tilde{\theta}) = (\gamma^2)^{-(\frac{n}{2}+a_\gamma)-1} \cdot \exp\left(-\frac{1}{\gamma^2} \left\{ \frac{1}{2}(\log(X)_{(n)} - \mu_{n,\phi,\tilde{\theta}}(\tilde{\gamma}^2))T_n^{-1}(\log(X)_{(n)} - \mu_{n,\phi,\tilde{\theta}}(\tilde{\gamma}^2))^T + b_\gamma \right\}\right),$$

which is proportional to an inverse gamma density on γ^2 dependent on $\tilde{\gamma}^2$. In the next we use the star (*) to denote values of the parameters sampled during the MCMC iterations, including the starting values. The MH step in the k th iteration of the MCMC begins with drawing a candidate value γ_{cand}^2 from the proposal density

$$\gamma_{\text{cand}}^2 \sim q(\gamma^2|\gamma_{k-1}^{2*}, \phi_k^*, \tilde{\theta}_k^*),$$

which is accepted with probability

$$\begin{aligned} & \min \left\{ 1, \frac{p(\gamma_{\text{cand}}^2 | \log(X)_{(n)}, N_{(n)}, \phi_k^*, \tilde{\theta}_k^*)q(\gamma_{k-1}^{2*} | \gamma_{\text{cand}}^2, \phi_k^*, \tilde{\theta}_k^*)}{p(\gamma_{k-1}^{2*} | \log(X)_{(n)}, N_{(n)}, \phi_k^*, \tilde{\theta}_k^*)q(\gamma_{\text{cand}}^2 | \gamma_{k-1}^{2*}, \phi_k^*, \tilde{\theta}_k^*)} \right\} \\ = & \min \left\{ 1, \exp\left(\frac{1}{2} \left(\frac{1}{\gamma_{k-1}^{2*}} + \frac{1}{\gamma_{\text{cand}}^2} \right) \right. \right. \\ & \left. \left. \cdot \left((\gamma_{k-1}^{2*} - \gamma_{\text{cand}}^2)t_{(n)}T_n^{-1}C_n^T + \frac{1}{4}((\gamma_{k-1}^{2*})^2 - (\gamma_{\text{cand}}^2)^2)t_{(n)}T_n^{-1}t_{(n)}^T \right) \right) \right\} \end{aligned}$$

with $C_n := \log(X)_{(n)} - \log(x_0)1_n - \phi_k^*t_{(n)} - \tilde{\theta}_k^*N_{(n)}$.

The full calculation can be seen in Hermann *et al.* (2016).

Because of the gamma conjugate prior for λ , it follows that $\lambda|N_{(n)} \sim \mathcal{G}(a_\lambda + N_{t_n} - N_{t_0}, b_\lambda + t_n - t_0)$.

All full conditional posteriors depend on the vector $N_{(n)}$ from the Poisson process. In many applications, including our own, this process is not observed. Therefore, this variable has to be generated from the actual observations within the Gibbs sampler. Since multivariate sampling is always a challenge, we will reduce the problem to sampling the independent differences $\Delta N_i = N_{t_{i+1}} - N_{t_i} \sim \mathcal{P}(\lambda\Delta t_i)$, given $\Delta t_i = t_{i+1} - t_i$. It is

$$\begin{aligned} \Delta \log(X)_i & := \log(X_{t_{i+1}}) - \log(X_{t_i}) | \Delta N_i, \phi, \gamma^2, \tilde{\theta} \\ & \sim \mathcal{N}\left(\left(\phi - \frac{\gamma^2}{2}\right) \Delta t_i + \tilde{\theta} \Delta N_i, \gamma^2 \Delta t_i\right). \end{aligned}$$

Therefore, the posterior density for ΔN_i is given by

$$\begin{aligned} & p(\Delta N_i | \Delta \log(X)_i, \phi, \gamma^2, \tilde{\theta}, \lambda) \\ \propto & \frac{\exp(-\lambda\Delta t_i)}{(\Delta N_i)!} \frac{1}{\sqrt{2\pi\gamma^2\Delta t_i}} \\ & \exp\left(-\frac{1}{2\gamma^2\Delta t_i} \left(\Delta \log(X)_i - \left(\phi - \frac{\gamma^2}{2}\right) \Delta t_i - \tilde{\theta} \Delta N_i \right)^2 + \Delta N_i \log(\lambda\Delta t_i)\right), \end{aligned}$$

which is not recognized as a member of a known distribution family. We propose the following sampling procedure for the k th iteration:

- for all $i = 1, \dots, n - 1$, choose $R \in \mathbb{N}$ (large enough) for the candidate set $\{0, \dots, R\}$
- calculate the posterior probabilities p_0, p_1, \dots, p_R with

$$p_j = p(j | \Delta \log(X)_i, \phi_{k-1}^*, \gamma_{k-1}^{2*}, \tilde{\theta}_{k-1}^*, \lambda_k^*), j = 0, 1, \dots, R$$

- draw $u \sim \mathcal{U}(0, \sum_{j=0}^R p_j = 1)$ and calculate $m = \min\{r : \sum_{j=0}^r p_j \geq u\}$
- set $\Delta N_i^k = m$.

Additionally, set $N_{(n)}^k = (0, \Delta N_1^k, \dots, \sum_{i=1}^n \Delta N_i^k)$.

All the distributions involved in the Gibbs sampler can be summarized as follows, for each iteration $k = 1, \dots, K$:

$$\begin{aligned} N_{(n)}^k &\sim p(N_{(n)} | \log(X)_{(n)}, \phi_{k-1}^*, \gamma_{k-1}^{2*}, \tilde{\theta}_{k-1}^*, \lambda_{k-1}^*) \\ \lambda_k^* &\sim p(\lambda | N_{(n)}^k) \\ \phi_k^* &\sim p(\phi | \log(X)_{(n)}, N_{(n)}^k, \tilde{\theta}_{k-1}^*, \gamma_{k-1}^{2*}) \\ \tilde{\theta}_k^* &\sim p(\tilde{\theta} | \log(X)_{(n)}, N_{(n)}^k, \phi_k^*, \gamma_{k-1}^{2*}) \\ \gamma_k^{2*} &\sim p(\gamma^2 | \log(X)_{(n)}, N_{(n)}^k, \phi_k^*, \tilde{\theta}_k^*). \end{aligned} \quad (5)$$

5 Some critical issues about model and choice of priors

From

$$\begin{aligned} \mathbb{E}[\log(X_t) | \phi, \gamma^2, \tilde{\theta}, \lambda] &= \log(x_0) + \left(\phi - \frac{\gamma^2}{2} \right) t + \tilde{\theta} \lambda t \\ &= \log(x_0) + \left((\phi + \tilde{\theta} \lambda) - \frac{\gamma^2}{2} \right) t \end{aligned} \quad (6)$$

it can be seen that there is a potential identifiability problem due to $\tilde{\theta}$ and λ , related to size and number of jumps, respectively. Such issue cannot be resolved joining the two parameters since the resulting stochastic process would be intractable, taking values only on multiples of the unknown quantity $\tilde{\theta}$. Inference for a simulated series will give a good overview of the resulting consequences and will provide a way to manage the issue, which will be used successfully later to analyze the cylinder liner data.

Simulation

In the real data set of the cylinder liners, we observe the wear process in several independent series, corresponding to measurements over time in 30 cylinders. We assume them to be realizations of the same process in (2) so that the likelihood is obtained by multiplying the likelihoods for all 30 cylinders, which share the same parameters. No information is provided about possible different behaviors of the cylinders (e.g., in a freight or in a passenger ship) so that we can assume their wear processes can be modeled with the same SDE, similarly to the other papers using those data. The use of data from 30 cylinders compensate also the scarcity of observations for each of them (ranging from 1 to 4).

Therefore, we simulate 10 series of the process (2) in $t_0 = 0, \dots, t_{101} = 5$, i.e. at points equispaced by 0.05, with $\phi = -0.05$, $\tilde{\theta} = -0.2$, $\gamma^2 = 0.05^2$ and $\lambda = 2$. We consider the simulated data as coming from the same model and we construct a likelihood function based on all of them. We repeated the simulation study with different values and the findings were similar to the ones reported here.

We present first the simulation study and then the analysis of the real data. The choice of the prior distributions will be the same in both cases, to make them similar as much as possible. Since no expert knowledge is available for eliciting the parameters, diffuse priors will be used. We take

$$m_\phi = 0, v_\phi = 1, m_\theta = 0, v_\theta = 1,$$

so that the prior means and the variances of ϕ and $\tilde{\theta}$ will be 0 and 1, respectively. We take

$$a_\gamma = 2 + 10^{-10}, b_\gamma = 10^{-5}, a_\lambda = 1, b_\lambda = 0.1,$$

so that $\mathbb{E}[\gamma^2] = \frac{b_\gamma}{a_\gamma - 1} = \frac{10^{-5}}{1 + 10^{-10}} \approx 10^{-5}$ and

$$Var(\gamma^2) = \frac{b_\gamma^2}{(a_\gamma - 1)^2(a_\gamma - 2)} = \frac{10^{-10}}{(1 + 10^{-10})^2 \cdot 10^{-10}} = \frac{1}{(1 + 10^{-10})^2} \approx 1,$$

whereas $\mathbb{E}[\lambda] = \frac{a_\lambda}{b_\lambda} = 10$ and $Var(\lambda) = \frac{a_\lambda}{b_\lambda^2} = 100$.

The choice of means equal, or close, to 0 for ϕ , $\tilde{\theta}$ and γ , denotes that, a priori, we give a negligible value to the drift of the process, the size of the jumps due to the soot particles and the contribution by the corrosive action modeled via the Wiener process. We believe such choices are somehow justified by the physical process where corrosion and contribution by a single soot particle are minimally affecting the wear and we should expect a very negligible trend. At the same time we expect quite a number of interactions between soot particles and liner so that the expected value of the jump process is quite away from 0. Although we start from those prior means, we strongly attenuate our assessments by considering large variances, allowing for posterior estimates, e.g. means, to be mostly driven by data.

We would like to study the influence of the starting points on estimation and prediction, considering two scenarios, representative of many simulations we did. First, we consider significantly perturbed starting values, with respect to the actual ones, multiplying the latter ones by 5, so that

$$\phi_0^* = 5 \cdot \phi, \quad \tilde{\theta}_0^* = 5 \cdot \tilde{\theta}, \quad \gamma_0^{2*} = 5 \cdot \gamma^2, \quad \lambda_0^* = 5 \cdot \lambda. \quad (7)$$

Later, we start from the right values of ϕ and γ^2 but we significantly perturb $\tilde{\theta}$ (multiplying the real value by 5) and λ (dividing it by 5). In this way we have different values with respect to the original ones but their product is unchanged. This choice allows us to see the consequences of the identifiability problem posed by (6). Therefore, we take

$$\phi_0^* = \phi, \quad \tilde{\theta}_0^* = \frac{1}{5} \cdot \tilde{\theta}, \quad \gamma_0^{2*} = \gamma^2, \quad \lambda_0^* = 5 \cdot \lambda \quad (8)$$

and we look for the estimates, especially of $\tilde{\theta}$ and λ , to see if they differ from the original values, denoting possible local maxima of the posterior distribution.

We will find out that the identifiability issue is affecting estimation, whereas it is no more a problem when considering predictions.

Starting from the values in (7), we can see the chains resulting from the Gibbs sampler presented in (5) in Figure 1, where the red lines mark the true values. Although the starting values are quite far from the true ones, the chains move quickly to a stationary distribution that provides estimates of the parameters very close to the real ones, with just a small underestimation for λ .

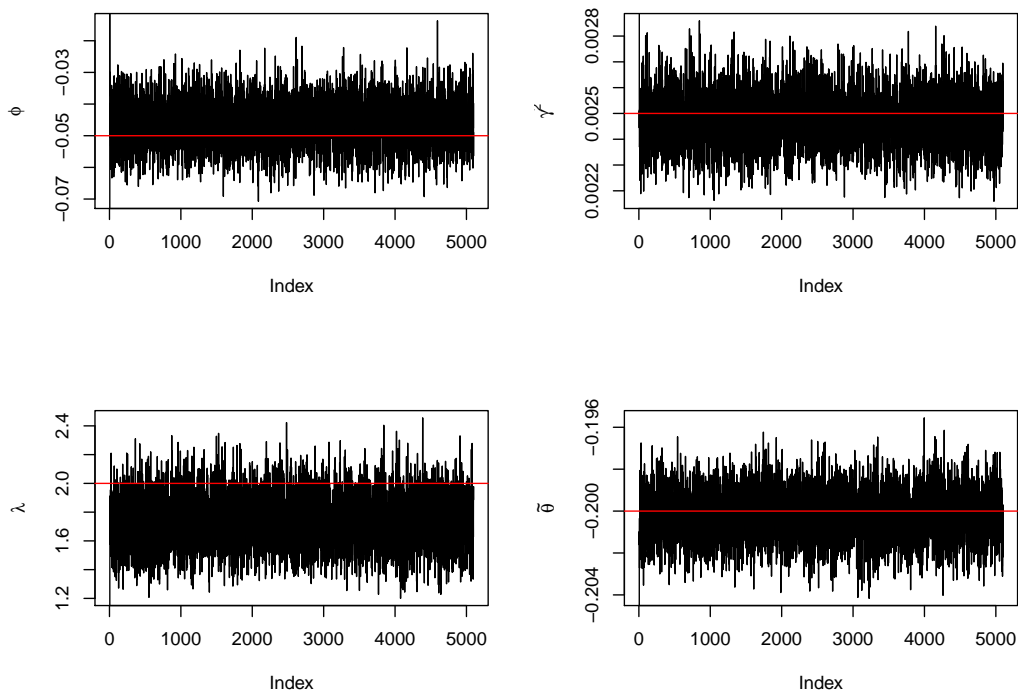


Figure 1: Markov chains for the simulated series with starting values (7), compared with the true parameter values (red lines).

Therefore, this procedure works in the case of starting values significantly away from the right ones, even with diffuse prior specification. As mentioned before, with regard to the identifiability problem posed by (6), we should investigate what happens if we start the algorithm from the values in (8). In Figure 2 we can see the Markov chains from the Gibbs sampler which run into a local optimum where we get stationary chains. In Figure 3, we compare the posterior densities with the two different sets of starting values. We can notice no remarkable difference for ϕ and γ^2 whereas $\hat{\theta}$ and λ are quite far apart, although their product is not changing much.

We can state that the algorithm is sensitive against the choice of starting values. Further examples were done by the authors, even with priors with true parameters as means and standard deviations equal to their absolute value. It is worth mentioning here that, in the case of prior means equal to the values in (8), prior standard deviation equal to the corresponding absolute values and starting values in (7), we still obtained biased estimations. We saw that

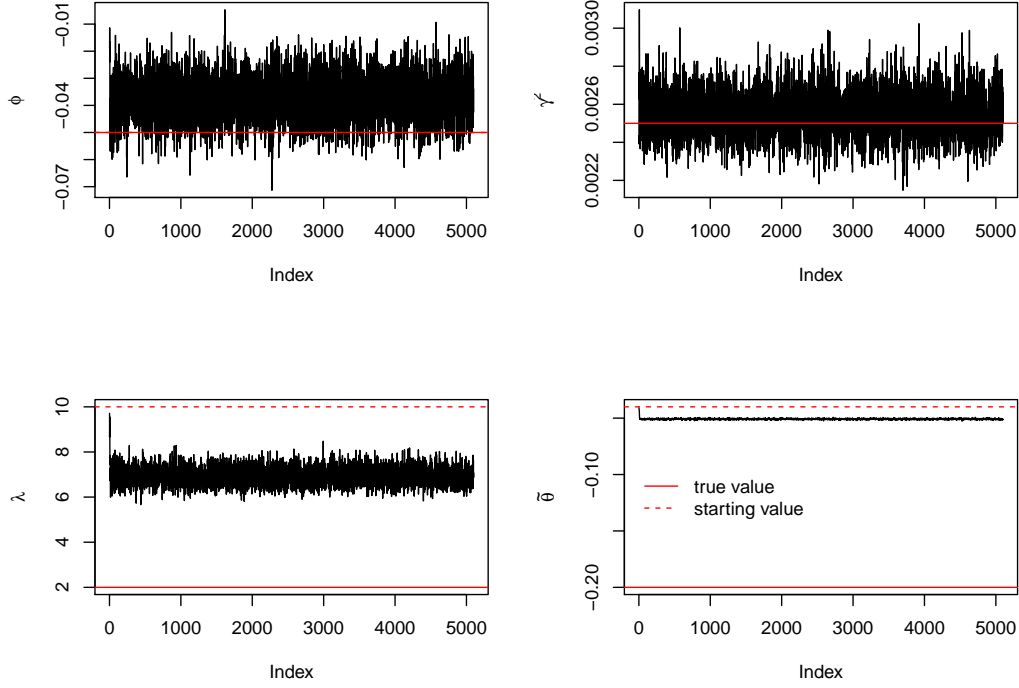


Figure 2: Markov chains for the simulated series with prior mean equal to the true values and starting values as in (8).

no significant change was induced by considering less diffuse priors, so that our estimation is not affected by the lack of information which is driving our decision of considering diffuse priors for the real data, as discussed earlier.

In many applications, one is not only interested in the estimation of model parameters but also in predictions about future experiments. The predictive distribution for the process at a future time t^* can be calculated as follows:

$$\begin{aligned}
 p(\log(X_{t^*}) | \log(X)_{(n)}) &= \int p(\log(X_{t^*}) | N_{t^*}, \phi, \tilde{\theta}, \gamma^2) \cdot \\
 &\quad p(N_{t^*}, \phi, \tilde{\theta}, \gamma^2 | \log(X)_{(n)}) d(N_{t^*}, \phi, \tilde{\theta}, \gamma^2) \\
 &\approx \frac{1}{K} \sum_{k=1}^K p(\log(X_{t^*}) | N_{t^*}^k, \phi_k^*, \tilde{\theta}_k^*, \gamma_k^{2*})
 \end{aligned} \tag{9}$$

with

$$\begin{aligned}
 N_{t^*}^k \sim p(N_{t^*} | \log(X)_{(n)}) &= \int p(N_{t^*} | \lambda) p(\lambda | \log(X)_{(n)}) d\lambda \\
 &\approx \frac{1}{K} \sum_{k=1}^K p(N_{t^*} | \lambda_k^*),
 \end{aligned}$$

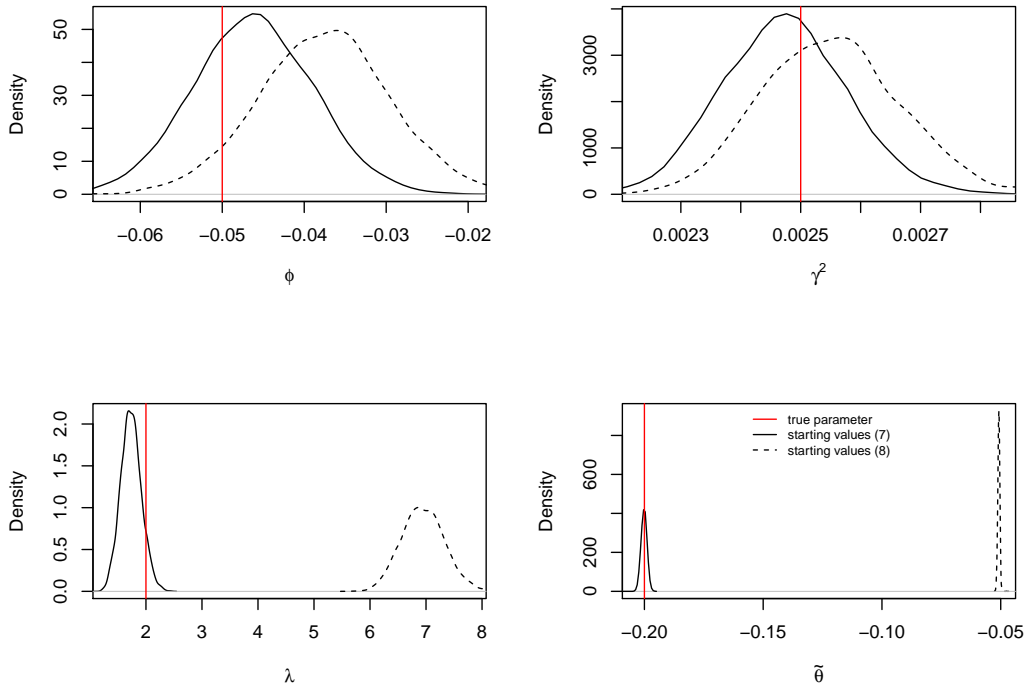


Figure 3: Posterior densities resulting from the MCMC started with (7) (black solid lines) and (8) (dotted lines), compared with the true parameters (red).

where ϕ_k^* , $\tilde{\theta}_k^*$, γ_k^{2*} and λ_k^* are samples from the posterior distribution resulting from the Gibbs sampler (5). Sampling from (9) yields to the $(1 - \alpha)$ -prediction interval on X_{t^*} by taking the $\frac{\alpha}{2}$ - and $(1 - \frac{\alpha}{2})$ -quantiles as lower and upper bounds.

Figure 4 displays the prediction results based on the Markov chains in Figures 1 and 2, each with a burn-in phase of the first 500 samples. The solid red lines show the pointwise 95% prediction intervals based on arbitrarily chosen starting values (7) (see Figure 1), which are larger than the dotted red lines which mark the prediction intervals based on the starting values chosen as in (8), see Figure 2. On average, 98% of the prediction intervals based on the samples in Figure 1 cover the corresponding simulated data point. In comparison, only 80% of the other (dotted) prediction intervals cover the true points.

Hence, the prediction result is a good classification quantity to decide between different starting values. We could base the analysis of the wear data on this finding, but we prefer a more sound approach stemming from all the findings from the simulated data, which will lead to satisfactory results, as shown in the next section.

Given that we found out from our simulations that estimation was not significantly affected by the choice of the priors but mostly by the starting values, especially those of $\tilde{\theta}$ and λ , we have been looking for a strategy allowing us to cope with the identifiability problem in (6). We propose a method which considers a broad grid of starting points, performs the Bayesian analysis through the Gibbs sampler presented in (5) and then considers the credible intervals obtained from all the chains, removes those containing unacceptable values (i.e. positive ones

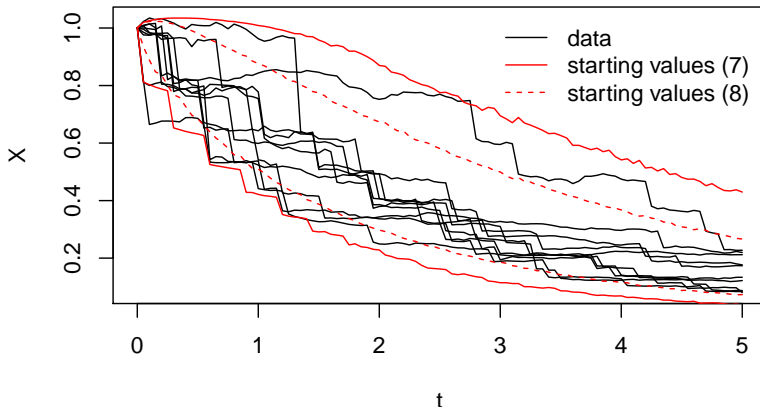


Figure 4: Comparison of the 95% prediction intervals with starting values (7) (solid) and (8) (dotted).

for ϕ and $\tilde{\theta}$) and estimates the parameters.

Application to the thickness data

As mentioned earlier, wrong starting values and wrong informative prior specifications can lead to biased estimations. Since no expert knowledge is available about the parameters, we use the same diffuse prior specification as in the previous simulation study:

$$m_\phi = 0, v_\phi = 1, m_\theta = 0, v_\theta = 1, a_\gamma = 2 + 10^{-10}, b_\gamma = 10^{-5}, a_\lambda = 1, b_\lambda = 0.1.$$

As we have seen in the simulation, the algorithm is sensitive against the starting values. Therefore, we have to investigate the behavior of the Gibbs sampler under different starting values. We take four values for each parameter:

$$\begin{aligned} \phi_0^* &\in \{-10^{-5}, -10^{-4}, -10^{-3}, -10^{-2}\}, & \tilde{\theta}_0^* &\in \{-10^{-5}, -10^{-4}, -10^{-3}, -10^{-2}\}, \\ \gamma_0^{2*} &\in \{5 \cdot 10^{-7}, 10^{-6}, 10^{-5}, 10^{-4}\}, & \lambda_0^* &\in \{0.25, 1, 5, 10\} \end{aligned}$$

and expand a four-dimensional grid, which has 256 sets of starting values. For each of them, the Gibbs sampler is implemented and an example of the corresponding chains can be seen in Figure 5.

In Figure 6, we see (in black) the 256 resulting 95% credible intervals, calculated by the 0.975 and 0.025 quantiles of Markov chain samples of size 1,000, obtained after drawing 6,500 iterations with a burn-in phase of 1,500 and a thinning rate of 5; the points mark the medians of each posterior distribution. The corresponding starting values are presented in red. It is evident that there is a lot of stability in the obtained credible intervals, despite the broad range of starting values.

Because of the thickness problem at hand, we know that ϕ and $\tilde{\theta}$ have to be negative. Therefore, we rule out the chains which lead to a positive 0.975 quantile for any of such

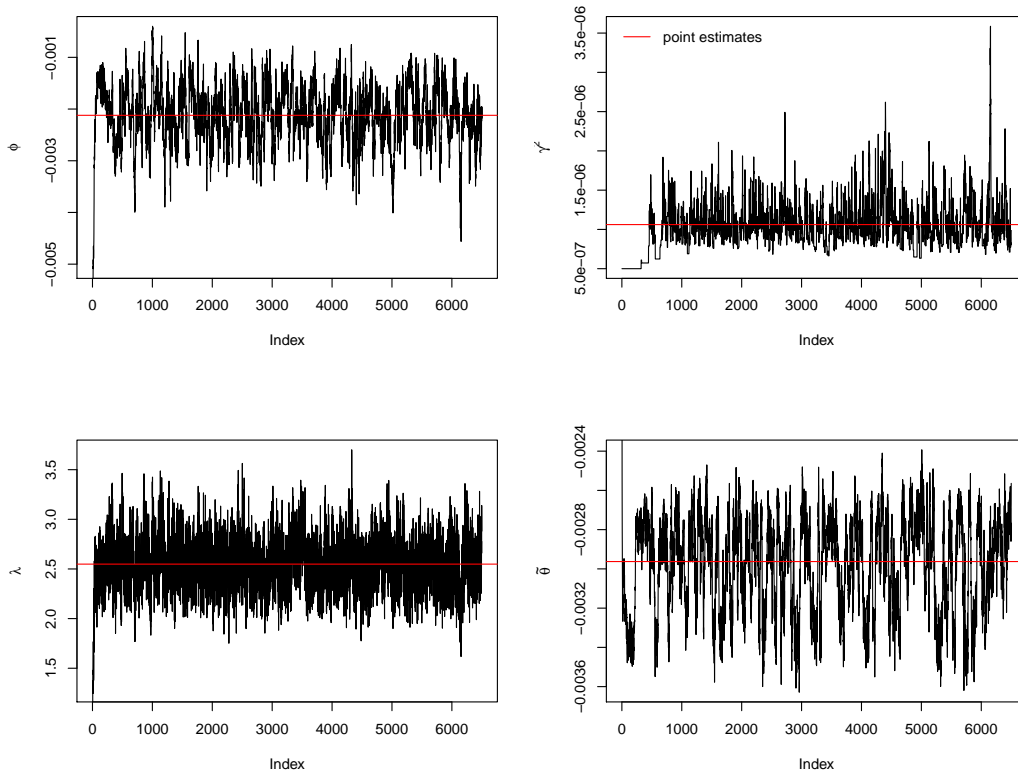


Figure 5: Example of Markov chains for a starting point: $\phi_0^* = -10^{-5}$, $\tilde{\theta}_0^* = -10^{-5}$, $\gamma_0^{2*} = 5 \cdot 10^{-7}$, $\lambda_0^* = 0.25$.

parameters, and we get the corresponding picture in Figure 7. The first credible interval in Figure 7 corresponds to the chains presented in Figure 5. Most of the 238 remaining chains lead to very similar credible intervals, where the minor deviation can be the result of the approximation by a sample of size 1,000. There are a few outliers among the intervals for λ and $\tilde{\theta}$ which will equalize each other in the predictive distribution. Thus, we put all the remaining chains together one after another. These 238×1000 samples approximate the posterior distribution and lead to the following estimates of the posterior means:

$$\hat{\phi} = -2.12 \cdot 10^{-3}, \quad \hat{\tilde{\theta}} = -2.96 \cdot 10^{-3}, \quad \hat{\gamma}^2 = 1.06 \cdot 10^{-6}, \quad \hat{\lambda} = 2.55. \quad (10)$$

Looking at the expected value of $\log(X_t)$ in (6) and plugging in the estimates in (10), it can be seen that $\hat{\tilde{\theta}}\hat{\lambda}$ is the most influential term, as expected, since it is the result of the wear due to soot particles whereas the corrosive activity, represented by $\hat{\gamma}^2$, is quite negligible.

The estimated parameters in (10) are used to calculate the predictive distribution in (9). The 0.025- and 0.975- quantiles provide pointwise 95% prediction intervals. In Figure 8 we see the 95% prediction intervals for the data set: only three points are not covered, which yields a coverage rate of 0.948 which is approximately 95%.

The 95% prediction interval in Figure 8 is based on data from 30 cylinders and it can be used to assess a maintenance policy for a cylinder with a new liner. Upon installation of the

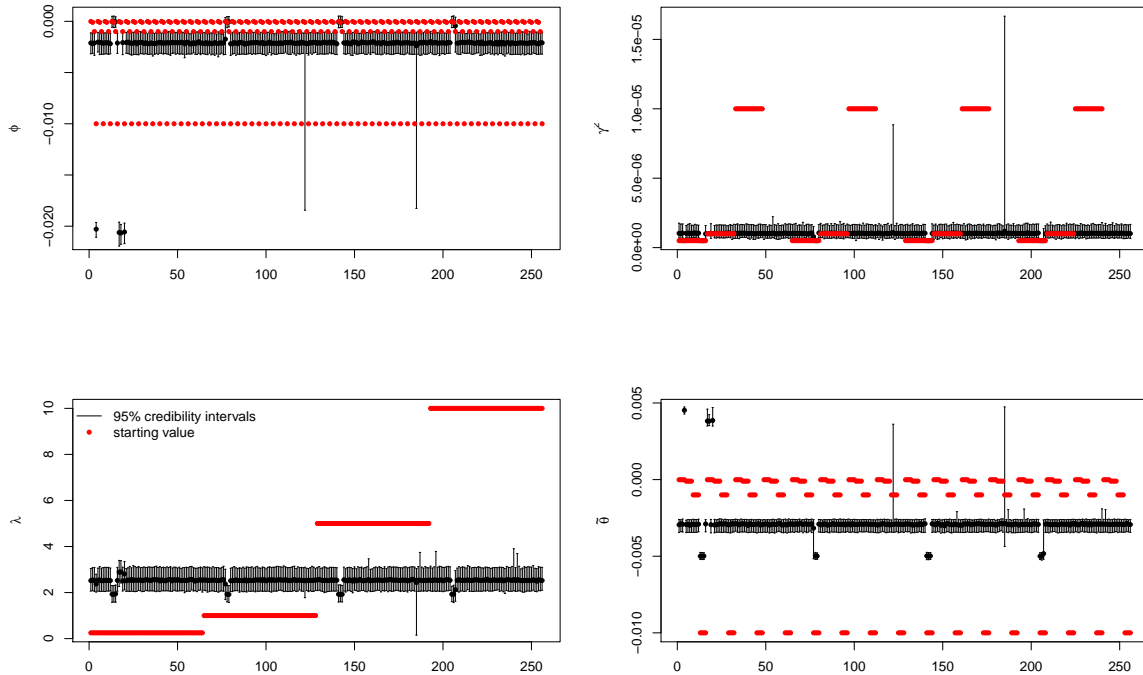


Figure 6: Credible intervals for 256 different starting values (in red).

new liner, the ship owner might decide to set some thresholds (e.g. 98 or 97 millimeters) when maintenance should be performed. A conservative procedure would be to perform maintenance as soon as the credible interval contains such values (here approximately at 1.2 and 1.8, respectively).

The maintenance policy for a cylinder in which wear has already been measured in the past is just slightly different: prediction of the wear behavior is still possible using the posterior distribution of the parameters but the initial thickness will not be 100 millimeters but the last measured value. We performed such analysis for two cylinders, namely the first and the fifth in the data, whose thickness was measured at three different times. To check the predictive performance, we considered thickness and time at which the second measurement was taken, i.e., 98.7 millimeters at time 1.468 for the first cylinder and 97.75 millimeters at time 1.87 for the fifth cylinder. Then we considered the predictive intervals (using green for first and blue for fifth cylinder) for the future behavior of the thickness in Figure 9 and we showed that the third, actual measurements are well inside the intervals. As before, maintenance could be performed as soon as the prediction interval contains a threshold value. In alternative, maintenance could be performed at a time τ when the probability of thickness below a given threshold ρ gets larger than a fixed value α , i. $P(X_\tau \leq \rho) \geq \alpha$. As an example about the considered cylinders, we have that the probability of getting a thickness smaller than 97 millimeters at time 3 is 0.298 for the first cylinder and 0.704 for the fifth one, showing a more critical situation for the latter.

These findings are useful for our future research about optimal maintenance policies.

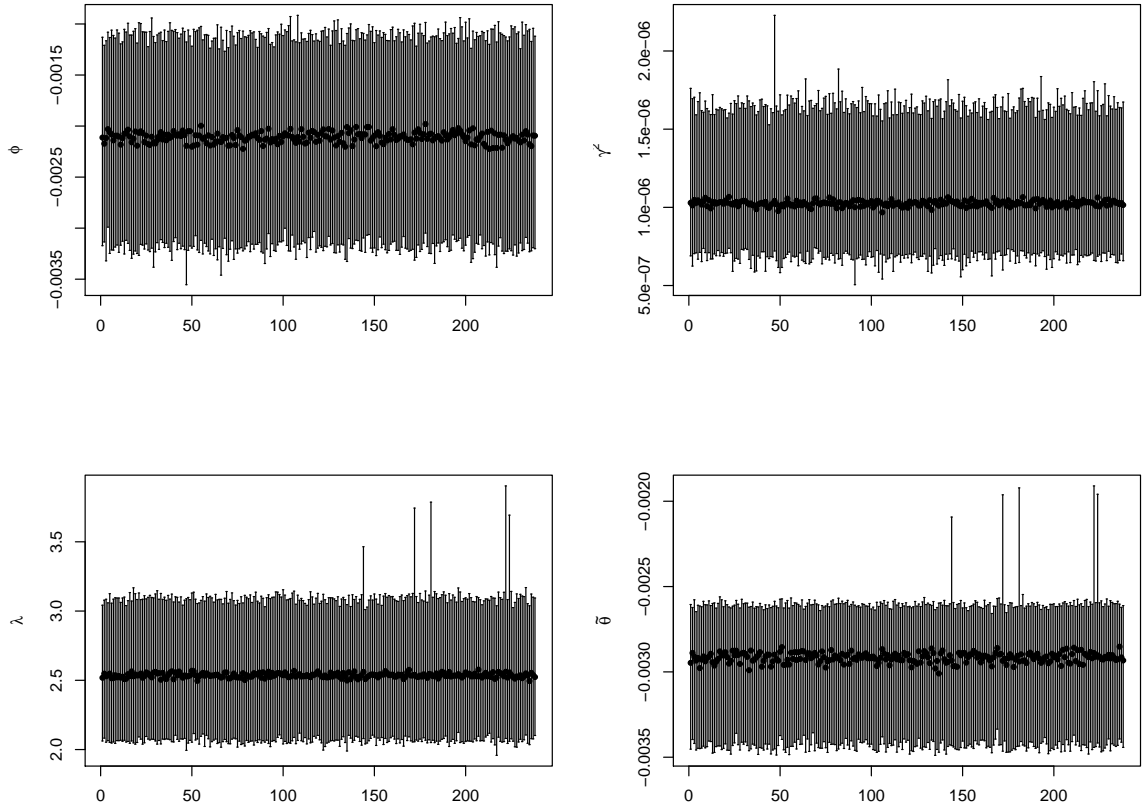


Figure 7: Credible intervals for starting values leading to nonpositive 95% prediction intervals.

In Figure 10 we compare the observed data with simulated ones generated from the posterior means. We can see that the data show a moderate nonlinear, convex behavior which can be observed only slightly in the simulations.

An extension that could provide more evident convex trajectories might be obtained considering N_t as a nonhomogeneous Poisson process (NHPP) with intensity function $\lambda(t) = ae^{-bt}$, $a, b > 0$. This NHPP would allow us to model even better the decrease of the wear increment with respect to the wear, allowing for less and less jumps. The possible improvement in forecasting trajectories comes at the price of an ever larger computational complexity. We decided that the use of a homogeneous Poisson process (HPP) represents a good trade-off between computational complexity and accurate estimation/forecast.

6 Discussion

The paper proposes a model, based on a jump diffusion process, whose mathematical aspects can find a physical justification in the analysis of the wear of cylinder liners in a marine diesel engine. The model could be applied for other wear degradation cases, as well. Different issues, like identifiability of parameters, are raised when using the model and a simulation study has

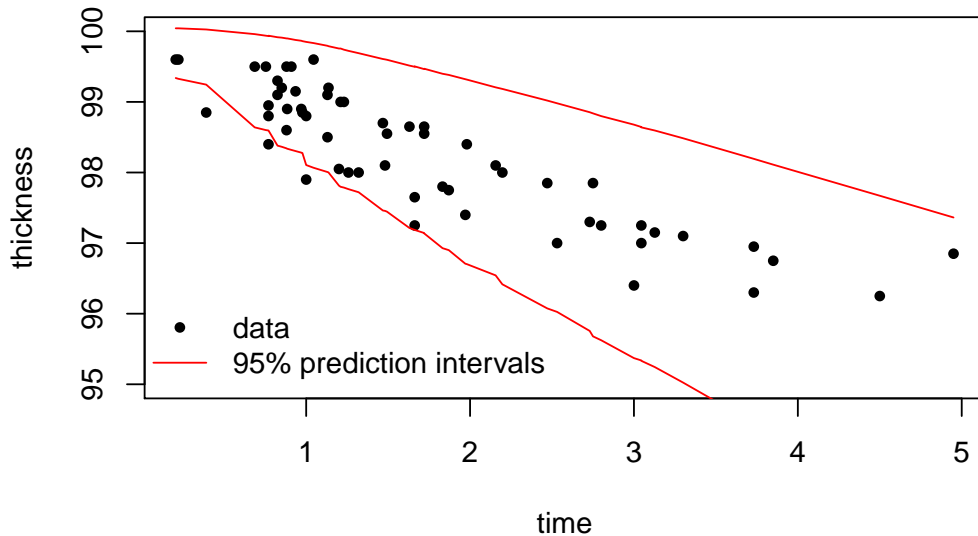


Figure 8: 95% prediction interval (red lines) for the wear data compared with actual data (black).

been performed to better understand them and propose a method which works satisfactorily when applied to real data. A different approach could have been taken; it is based on how well the estimated model can forecast the actual data, choosing the estimated parameters which lead to predictive intervals covering the largest number of observed data. We are willing to pursue research in such direction in the future, but, for the moment, we found that our current strategy is quite robust with respect to different choices of priors and starting points in the MCMC simulation and leads to satisfactory results, in terms of estimation and forecast.

Further work will be devoted to consider jumps modeled with nonhomogeneous Poisson processes since their number might be decreasing over time, as a consequence of the reduction in thickness decrease. The research should face the increased computational complexity.

Finally, the model will be used to develop optimal maintenance policy taking in account also the costs of inspection, missed liner replacement, stop of ship, etc.

Acknowledgements

The second author would like to thank Fernanda D’Ippoliti, Massimiliano Giorgio, Maurizio Guida and Gianpaolo Pulcini for the helpful discussions he had with them.

This work was financially supported by Project B5 “Statistical methods for damage processes under cyclic load” of the Collaborative Research Center “Statistical modeling of non-linear dynamic processes” (SFB 823) of the German Research Foundation (DFG).

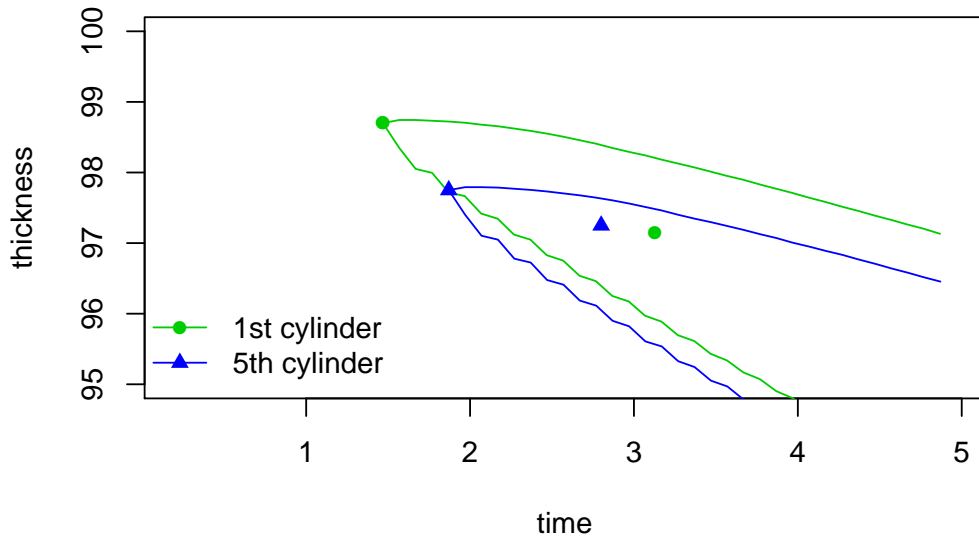


Figure 9: 95% prediction intervals for 1st (in green) and 5th (in blue) cylinders and comparison with future actual measurements (green circle and blue triangle, respectively).

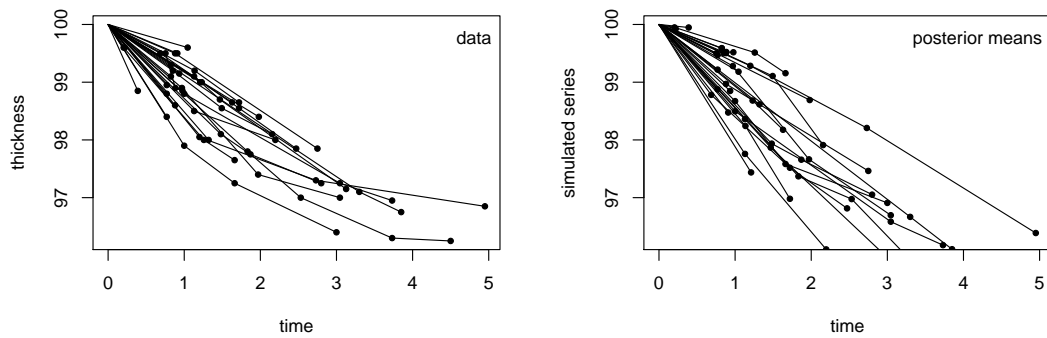


Figure 10: Comparison of observed data (left) and simulated trajectories using posterior means of parameters (right).

References

- Bocchetti, D., Giorgio, M., Guida, M. and Pulcini, G. (2006). A competing risk model for the reliability of cylinder liners in ship Diesel engines, in C. Guedes Soares and E. Zio (eds.), *Safety and Reliability for Managing Risk*, Taylor and Francis Group, London, pp. 2751–2759.

- D'Ippoliti, F. and Ruggeri, F. (2009). Stochastic modelling of cylinder liners wear in a marine diesel engine, *Mathematical Methods in Reliability 2009*, 161-163.
- Giorgio, M., Guida, M. and Pulcini, G. (2007). A Wear Model for Assessing the Reliability of Cylinder Liners in Marine Diesel Engines, *IEEE Transactions on Reliability*, Vol. 56, No. 7, pp. 158–166.
- Giorgio, M., Guida, M. and Pulcini, G. (2010). A State-Dependent Wear Model With an Application to Marine Engine Cylinder Liners, *Technometrics*, Vol. 52, No. 2, pp. 172-187.
- Giorgio, M., Guida, M. and Pulcini, G. (2011). An age- and state-dependent Markov model for degradation processes, *IIE Transactions*, Vol. 43, pp. 621–632.
- Giorgio, M., Guida, M. and Pulcini, G. (2015a). A new class of Transformed Gamma age- and state-dependent degradation processes with covariates, *IEEE Transactions on Reliability*, Vol. 64, No. 2, pp. 562–578.
- Giorgio, M., Guida, M. and Pulcini, G. (2015b). A condition-based maintenance policy for deteriorating units. An application to the cylinder liners of marine engine, *Applied Stochastic Models in Business and Industry*, Vol. 31, pp. 339-348.
- Hermann, S., Ickstadt, K. and Müller, C.H. (2016). Bayesian prediction for a jump diffusion process - with application to crack growth in fatigue experiments, *Submitted*.
- Moraes, A., Ruggeri, F., Tempone, R. and Vilanova, P. (2014). Multiscale modeling of Wear Degradation in Cylinder Liners, *Multiscale Modeling and Simulation*, Vol. 12, pp. 396–409.
- Øksendal, B. and Sulem, A. (2005). *Applied Stochastic Control of Jump Diffusions*, Springer, Berlin Heidelberg.

